

Automated classification of transient contamination in stationary acoustic data

Christopher J. Bahr^{a,*}, Todd Schultz^b

^a*Aeroacoustics Branch, NASA Langley Research Center, Hampton, Virginia, USA*

^b*Boeing Test & Evaluation, The Boeing Company, Seattle, Washington, USA*

Abstract

An automated procedure for the classification of transient contamination of stationary acoustic data is proposed and analyzed. The procedure requires the assumption that the stationary acoustic data of interest can be modeled as a band-limited, Gaussian random process. It also requires that the transient contamination be of higher variance than the acoustic data of interest. When these assumptions are satisfied, it is a blind separation procedure, aside from the initial input specifying how to subdivide the time series of interest. No a priori threshold criterion is required. Simulation results show that for a sufficient number of blocks, the method performs well, as long as the occasional false positive or false negative is acceptable. The effectiveness of the procedure is demonstrated with an application to experimental wind tunnel acoustic test data which are contaminated by hydrodynamic gusts.

Keywords: binary classification, noise contamination, unsupervised methods

Nomenclature

B	= normalized signal bandwidth
K	= Kullback-Leibler divergence
M	= Mach number
N	= number of samples in a block of data
n	= sample index
P	= probability distribution function
p	= probability density function
Q	= probability distribution function, estimate of P
q	= probability density function, estimate of p
y_n	= individual sample in a block of data
α	= gamma distribution shape parameter

*Corresponding author

Email address: christopher.j.bahr@nasa.gov (Christopher J. Bahr)

β	= gamma distribution scale parameter
Γ	= gamma function
γ	= incomplete gamma function
ν	= effective degrees of freedom of a signal of block size N
σ^2	= variance of a block of data
χ_N^2	= sum of the squares of the samples in a block of data

1. Introduction

IN aeroacoustic wind tunnel testing, experimentalists often seek to measure acoustic signals which can be modeled as band-limited, stationary random processes. The unfortunate reality for some experimental setups is that the acoustic signal of interest will be measured along with some form of contamination. For example, in an open-jet and acoustically-treated wind tunnel facility, the contamination observed by a microphone may manifest as either stationary pressure fluctuations generated by facility acoustic sources, or transient pressure fluctuations generated by flow over the microphone.¹ Stationary contamination may be mitigated through various forms of frequency domain background subtraction.^{2,3} However, such techniques are not appropriate for transient events.

Alternative analysis methods are required to classify and separate time domain contamination. While manual inspection of data is an option, this is usually impractical due to the large volume of data involved. This work presents an automated method which requires minimal input aside from the parameters to subdivide a given time series of interest. The identification and separation methodology has a well-defined parameter for classifying transient data, which should be valid as long as the underlying assumptions are approximately obeyed. It is assumed that the underlying acoustic signal of interest is a stationary, zero mean, Gaussian random process; and that the acoustic data of interest are of lower variance than transient contaminating data. These assumptions are addressed in more detail in the theoretical development of the classification technique in the following section. Subsequent sections evaluate the classification performance with both simulated and experimental data. These are followed by recommendations developed from the results.

2. Theoretical Development

The first assumption required for this transient classification procedure is that the underlying acoustic signal is a stationary, zero mean, Gaussian random process. If the samples from the acoustic signal of interest, y , are truly Gaussian-distributed random variables with zero mean and unit variance, then the sum

25 of the squares of a set of N samples,

$$\chi_N^2 = \sum_{n=1}^N y_n^2, \quad (1)$$

26 is a random variable which follows a chi-square distribution with N degrees of freedom.⁴ Dividing this
 27 relation by $N - 1$ expresses it in terms of the block variance with a known mean,

$$\sigma^2 = \frac{\chi_N^2}{N - 1} = \frac{1}{N - 1} \sum_{n=1}^N y_n^2, \quad (2)$$

28 which also follows a chi-square distribution.

29 It is relatively easy to enforce the zero mean condition on acoustic data, either through high-pass filtering
 30 during data acquisition or mean subtraction in post-processing. However the variance of the distribution for
 31 y is unknown, so a more general distribution is necessary to model the distribution of the block variance, σ^2 .
 32 As a generalization of the chi-square distribution, the gamma distribution can be used.⁵ The probability
 33 density function for a gamma distribution of the block variance (with a zero location parameter) is given by

$$p(\sigma^2) = \frac{1}{\beta \Gamma(\alpha)} \left(\frac{\sigma^2}{\beta} \right)^{\alpha-1} e^{-\frac{\sigma^2}{\beta}}, \quad (3)$$

34 where $\alpha = \nu/2$ is the shape parameter, β is the scale parameter and Γ is the gamma function

$$\Gamma(\alpha) = \int_0^{\infty} t^{\alpha-1} e^{-t} dt. \quad (4)$$

35 For $\beta = 2$, and substituting χ_N^2 for σ^2 , this collapses to the chi-square distribution. This scale parameter
 36 allows a distribution fit to handle nonunity variance of y .

37 In practice, the acoustic signal is not truly random white noise, but has a finite bandwidth and correlation
 38 timescale. This normalized bandwidth, B , alters the effective degrees of freedom, ν , of the signal.⁶ For
 39 example, a block of 8192 samples of a signal which is truly random has a spectrum of white noise and a
 40 bandwidth of 100%, so $\nu = N = 8192$. If the signal passes through an ideal lowpass filter set to 50% of the
 41 Nyquist frequency for the sampling rate, then $B = 0.5$ and the effective number of degrees of freedom is
 42 $\nu = B \times N = 4096$. This fractional, normalized bandwidth can be estimated through a simple procedure.
 43 First, the one-sided power spectral density of the signal must be computed. This function of frequency,
 44 $G_{yy}(f)$, must then be normalized such that its peak is unity,

$$G_{yy,\text{norm}}(f) = \frac{G_{yy}(f)}{\max[G_{yy}(f)]}. \quad (5)$$

45 The average of this normalized spectral density is then computed by integrating across the measurement
 46 bandwidth and normalizing by the integration range,

$$B = \frac{1}{f_{\text{max}}} \int_0^{f_{\text{max}}} G_{yy,\text{norm}}(f) df. \quad (6)$$

47 With the effective degrees of freedom and, thus, the shape parameter of a distribution fit derived from
 48 the signal bandwidth, the scale parameter must now be determined. An easy, if biased,⁷ estimate of β can
 49 be obtained from its maximum likelihood estimator

$$\beta = \frac{\overline{\sigma^2}}{\alpha}, \quad (7)$$

50 where $\overline{\sigma^2}$ is an estimate of the mean of the block variances. However, the mean of the variances is sensitive to
 51 extreme variance values, which may occur when a transient event is superimposed on the baseline Gaussian
 52 process. A statistical parameter that is less sensitive to extreme values is necessary for computing β . One
 53 such parameter is the median of the block variances. The median occurs where the probability distribution
 54 function is 0.5. The probability distribution function for the gamma distribution is given by

$$P(\sigma^2) = \frac{\gamma\left(\alpha, \frac{\sigma^2}{\beta}\right)}{\Gamma(\alpha)}, \quad (8)$$

55 where γ is the (non-normalized) incomplete gamma function⁵

$$\gamma\left(\alpha, \frac{\sigma^2}{\beta}\right) = \int_0^{\frac{\sigma^2}{\beta}} t^{\alpha-1} e^{-t} dt. \quad (9)$$

56 The equation for the median variance is thus

$$\frac{1}{2} = \frac{\gamma\left(\alpha, \frac{\sigma_{\text{med}}^2}{\beta}\right)}{\Gamma(\alpha)}. \quad (10)$$

57 Software libraries exist for efficiently inverting γ for a given α , thus yielding an estimate of the median
 58 variance normalized by β . The experimental median variance can then be divided by this estimate, yielding
 59 an estimate of β . Thus for a given shape factor α , two scale factors can be readily computed from the data.
 60 One, β_{mean} , is based on the mean of the block variances and may be significantly influenced by extreme
 61 values of block variance in the data such as may be present with transient events. The other, β_{median} , is
 62 based on the median of the block variances.

63 Having two scale factors allows for the construction of two gamma distributions. These can be compared
 64 to gain some sense of the relative influence of extreme block variances on the data set. Numerically this can
 65 be done by evaluating the Kullback-Leibler divergence, which is one metric for comparing distributions.⁸
 66 The divergence K is a measure of the information lost when probability distribution Q (or density q) is used
 67 to estimate distribution P (or density p). This is expressed as

$$K(p||q) = \int \ln \left[\frac{p(\sigma^2)}{q(\sigma^2)} \right] p(\sigma^2) d(\sigma^2). \quad (11)$$

68 While, in general, this can be difficult to compute, it is greatly simplified in the case of two gamma distri-
 69 butions with a common α . In this case, some manipulation yields

$$K(p||q)_{\alpha_p=\alpha_q=\alpha} = \alpha \left(\ln \beta_q - \ln \beta_p + \frac{\beta_p - \beta_q}{\beta_q} \right), \quad (12)$$

70 or, as used in this application,

$$K(p_{median}||p_{mean})_{\alpha_{median}=\alpha_{mean}=\alpha} = \alpha \left(\ln \beta_{mean} - \ln \beta_{median} + \frac{\beta_{median} - \beta_{mean}}{\beta_{mean}} \right). \quad (13)$$

71 The two distributions match when K is zero.

72 To summarize, two data distributions can be estimated. The distribution based on the block variance
73 mean is more sensitive to blocks with high variance, such as those containing transient contamination, than
74 the distribution based on block variance median. A metric is constructed for comparing the two distributions.
75 Now a procedure is proposed for determining which blocks of a given time series to retain and which to
76 reject. The process is illustrated in Fig. 1. It should be noted here that for the number of blocks traditionally
77 used in aeroacoustic wind tunnel testing, converged data distributions are not expected. The intent of the
78 following procedure is to provide an automated engineering tool to locate and thus exclude blocks in the
79 time series associated with transient events, not to accurately estimate the probability distribution of the
80 acoustic data block variance.

81 First, a given microphone time record is broken into blocks of a desired number of samples, N . This
82 value is usually dictated by the desired spectral estimation parameters. The variance of each of these blocks
83 is computed, and the blocks are sorted by their variance, from low to high. A minimum number of blocks is
84 selected to automatically accept as stationary. This number of blocks is taken as the lowest-variance subset
85 of blocks from the sorted set, and should be large enough to reduce the noise in the estimate but small
86 enough to avoid any extreme values, or contaminated blocks. Experience with simulations suggests 20% of
87 the total block count to be a safe selection, though a lower value was successfully used with experimental
88 data. This subset of blocks is used to compute an autospectral density, which can be used to calculate α .
89 This can be used to compute β_{mean} and β_{median} , followed by K . The next block, in order of ascending
90 variance, is added to the active subset of blocks and the process is repeated. This continues until all of
91 the blocks of data have been included, producing $|K|$ as a function of the number of blocks included in the
92 data set in order of ascending variance. The block set yielding the minimum $|K|$ is classified as stationary.
93 Blocks excluded from this set are classified as containing significant transient contamination. They may be
94 subsequently excluded from processing of the stationary data of interest.

95 3. Simulated Analysis

96 A simulation study is performed to measure the performance of the transient classification procedure
97 with data representative of experimental situations and parameter choices. The goal is to understand the
98 performance of the procedure for a variety of situations and to gain an understanding of how the algorithm
99 should perform for experimental data. Simulations are used as opposed to training data sets to better cover
100 a complete range of possible situations.

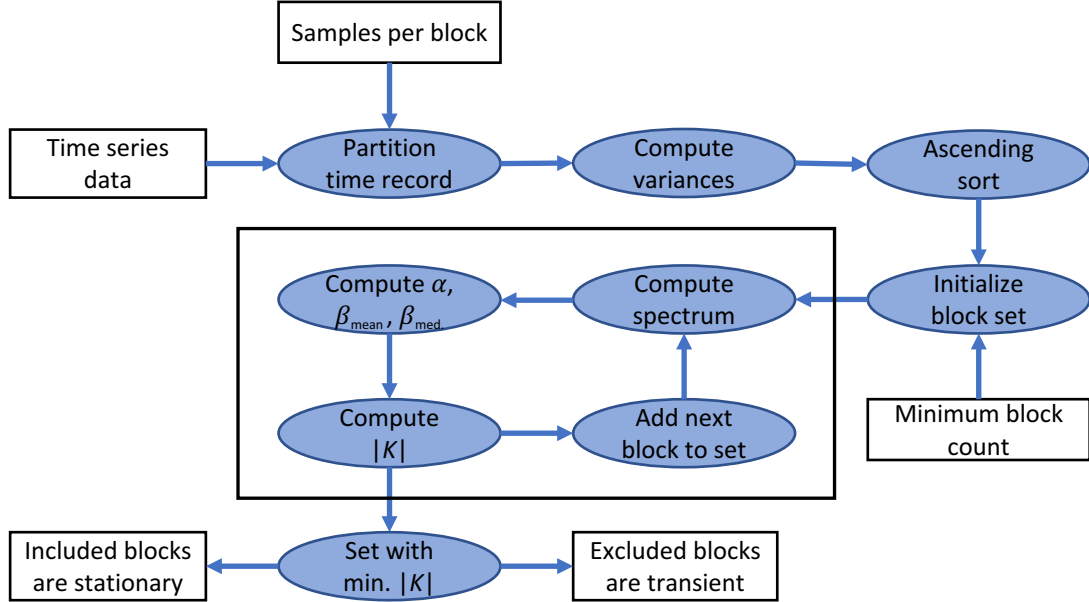


Figure 1. Algorithm flow chart for classifying transient events.

101 3.1. Performance metrics

102 Identification of a data block contaminated with noise is a binary classification problem where the data
 103 block is either a transient, contaminated block or a stationary, uncontaminated block. Thus, performance
 104 metrics used to evaluate binary classifiers can be used here.⁹ Note that for this study, classification of a
 105 data block as a transient, along with its subsequent rejection by the method and removal of the data block
 106 from the set of interest is considered as a positive result. The associated negative result is the classification
 107 of a data block as stationary. This study considers three performance metrics: accuracy, false positive rate,
 108 and false negative rate. The *accuracy* is the fraction of test cases that are correctly classified as either a
 109 transient data block or a stationary data block. The *false positive rate* is the fraction of the total number
 110 of stationary data blocks that are incorrectly classified as transient data blocks. It provides a measure of
 111 reduction in useful, stationary data blocks due to the classification process. The *false negative rate* is the
 112 fraction of the total number of transient blocks that are misclassified as stationary data blocks and provides
 113 a measure of the contaminated data blocks that are allowed through the algorithm.

114 An intermediate step for computing the accuracy, false positive rate, and false negative rate is the

115 calculation of the confusion matrix. For a binary classification problem, the confusion matrix is a two by
116 two table containing the counts of the classifier output for true positives and true negatives on the diagonal
117 elements and false positives and false negatives on the off-diagonal elements. Thus, the accuracy is the
118 sum of the diagonal elements divided by the total number of data blocks, while the false positive rate and
119 false negative rate are the off-diagonal elements divided by the total number of true or known positives or
120 negatives, respectively.

121 *3.2. Simulation cases*

122 The desired measured signal and the contamination signal are modeled as independent Gaussian noise
123 signals with different variances, with the variance of the contamination larger than the variance of the desired
124 signal. Five parameters are studied in simulations. These are the ratio of the variance of the contamination
125 to the variance of the signal, the total number of data blocks, the number of points N in each data block,
126 the percentage of the data blocks contaminated, and the percentage of the points in each data block that
127 are contaminated. For all simulation cases, the total number of data blocks is swept through values of 100,
128 200, 300, 400, 500, and 1,000. The remaining parameters are given in Table 1. These combinations yield a
129 total of 132 individual simulation cases.

130 *3.3. Simulation procedure*

131 The simulation procedure is as follows. First, a simulation case is selected, and the case parameters are
132 noted. Next, the non-contaminated signal is modeled as a unit variance Gaussian random signal with the
133 number of data points per data block and the number of blocks specified for the simulation case. Next,
134 the clean signal is divided into the desired number of blocks, with no block overlap. Then, the desired
135 number of blocks are contaminated for the desired percentage of points with additive noise specified by the
136 variance ratio and added to the first part of the block. The transient classification algorithm is applied
137 to the simulated data, and the data blocks classified as transients are logged. For these simulations, the
138 transient classification procedure automatically considers the 20% of data blocks with the lowest variance to
139 be stationary because lower total block counts approach the minimum necessary for a reasonable autospectral
140 estimate. The confusion matrix elements are then calculated and recorded. The process is repeated for a
141 total of 50,000 trials of data generation for each simulation case. The individual elements of the confusion
142 matrix are examined to ensure the mean and standard deviation have converged to within 0.1% based on
143 the values from one iteration to the next. Finally, the mean estimate for the confusion matrix is used to
144 compute the estimated mean accuracy, false positive rate, and false negative rate for the simulation case.

145 *3.4. Results*

146 Table 2 presents a statistical summary of the three performance metrics over all of the simulation cases.
147 The accuracy ranges from 80.1% to 99.3%. However, if the number of blocks is greater than or equal to 300,

Table 1. Parameter values for simulation cases. All cases sweep through six values of the total number of data blocks of 100, 200, 300, 400, 500, and 1000.

Variance ratio	Points per data block	Percentage of data blocks contaminated	Percentage of points in each data block contaminated
2	8192	75	100
2	8192	50	100
2	8192	25	100
2	8192	25	50
2	8192	25	25
2	8192	75	50
2	8192	75	25
2	2048	75	25
2	2048	75	100
2	2048	25	25
2	2048	25	100
3	8192	25	25
5	2048	25	100
5	2048	75	100
5	2048	25	25
5	2048	75	25
5	8192	75	25
5	8192	75	100
5	8192	25	25
5	8192	25	100
10	8192	25	25
100	8192	25	25

148 which is desirable for averaging of the spectral estimate as it approaches a normalized random error of 5%,
 149 the mean accuracy is greater than 90%. This condition also further constrains the false positive rate bounds
 150 to range from 0.9% to 12.9%, and the false negative rate bounds to range from 0.0% to 2.0%, improving on
 151 the results summarized in Table 2.

Table 2. Statistical summary of performance metrics for all simulation cases.

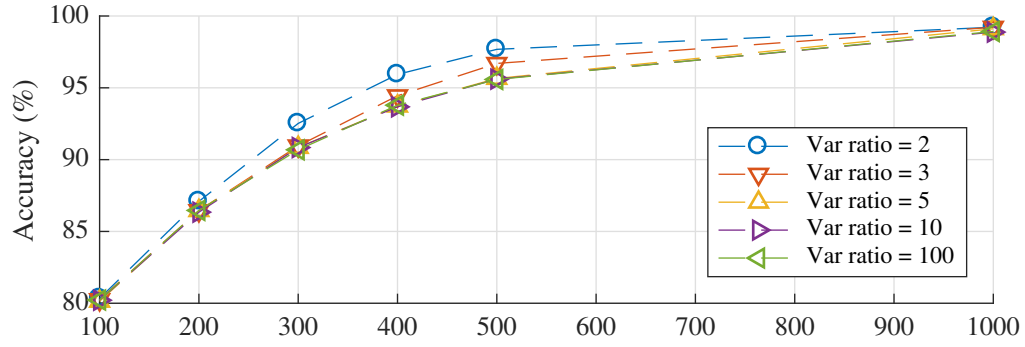
	Accuracy (%)	FPR (%)	FNR (%)
minimum	80.1	0.9	0.0
mean	94.4	8.8	0.3
median	97.0	6.2	0.01
maximum	99.3	26.4	4.2

152 *3.4.1. Number of data blocks and variance ratio*

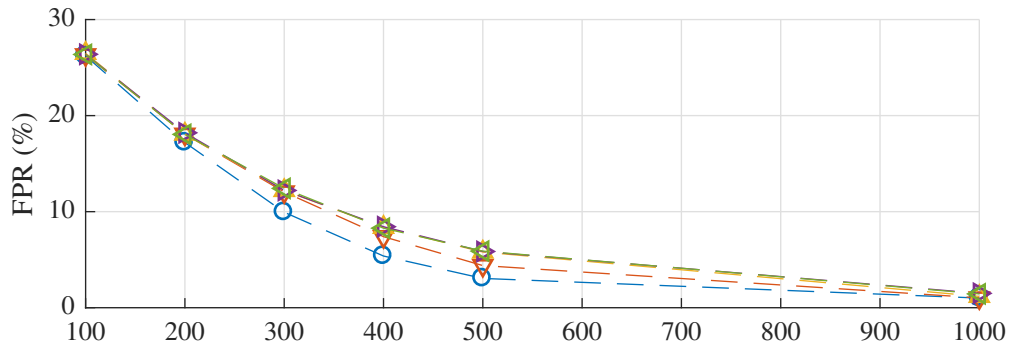
153 The variation in the performance of the algorithm is studied as a function of the total number of data
 154 blocks and contamination to signal variance ratio. Here, the number of data points per block was held to
 155 $N = 8,192$ points, the percent of contaminated blocks to 25%, and the percent of each contaminated block
 156 perturbed to 25%. This resulted in 30 simulation scenarios selected from the 132 total cases. The results, as
 157 plotted in Fig. 2, show that all performance metrics converge as a function of variance ratio when the ratio
 158 is greater than five. The accuracy and the false positive rate improve as the total number of data blocks
 159 increases. The false negative rate shows more variation, but the values are below 0.14% for all 30 scenarios.
 160 These rates correspond to total false negative counts of zero, one, or, at worst, two misclassified blocks.

161 *3.4.2. Percent of contaminated block perturbed*

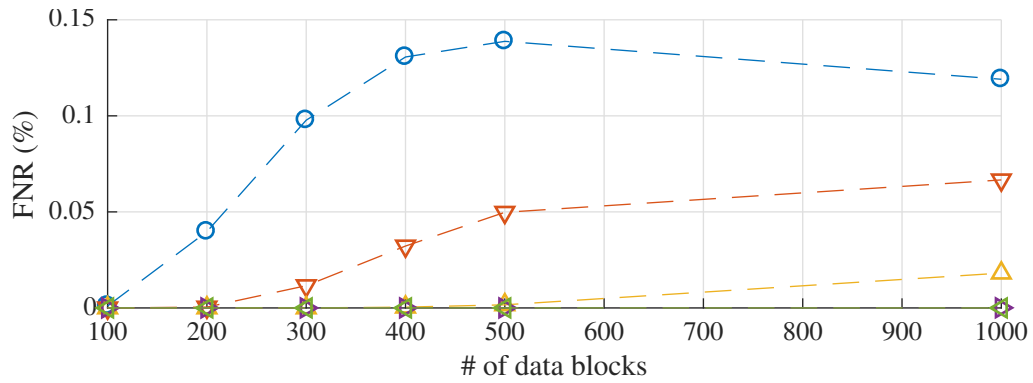
162 In the actual experiments analyzed in a subsequent section, transient gust contamination occurs spo-
 163 radically and for short durations. Thus, for any data block that is impacted, only a portion of that block
 164 may be contaminated. Understanding how sensitive the performance metrics are to the percentage of any
 165 given data block that is perturbed is critical to assessing the robustness of the method. This simulation
 166 subset held the variance ratio to 2 (the most challenging value in the simulation study), the number of data
 167 points per block to $N = 8,192$ points, and the percentage of contaminated blocks 25%. This resulted in
 168 18 simulation scenarios selected from the 132 total cases. The results, as plotted in Fig. 3, show that the
 169 accuracy and the false positive rate are minimally affected by the percentage of the contaminated data block
 170 that is perturbed, especially when compared to the impact from the total number of data blocks. The mag-
 171 nitudes of the correlation coefficients between the accuracy and percentage of the data block contaminated,
 172 and between the false positive rate and the percentage of the data block contaminated are less than 0.1,



(a) accuracy



(b) FPR



(c) FNR

Figure 2. Performance metrics varying the total number of data blocks and the contamination to signal variance ratio. The number of data points per block is held to to $N = 8,192$ points, the percentage of contaminated blocks to 25%, and the percent of each contaminated data block perturbed to 25%.

173 confirming the lack of a linear relationship as seen in Fig. 3. However, the false negative rate does show a
174 functional dependence on the percentage of the data block contaminated. This has a correlation coefficient
175 of -0.25 (p-value of 0.004). Thus, as the percentage of the data block that is contaminated increases, the
176 method can more easily identify data blocks that have been contaminated. However, the maximum false
177 negative rate is still only 0.14%.

178 3.4.3. *Percent of data blocks that are contaminated*

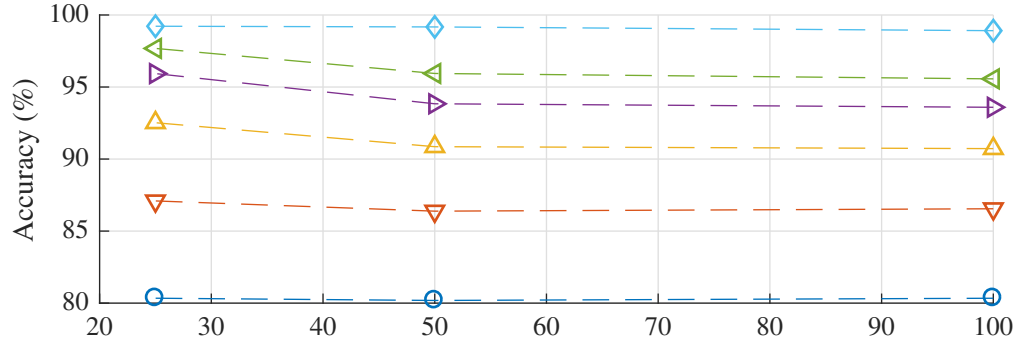
179 The variation in the performance of the classification algorithm is studied as a function of the percentage
180 of data blocks that are contaminated. This simulation subset held the variance ratio to 2, the number of
181 data points per block to $N = 8,192$ points, and the percent of each contaminated block perturbed to 25%,
182 resulting in 18 simulation scenarios selected from the 132 total cases. The results, as plotted in Fig. 4, show
183 that the accuracy and false positive rate improve with an increasing percentage of transient blocks in the
184 total data set, whereas the false negative rate worsens. The values of all three performance metrics as a
185 function of the percentage of contaminated blocks present in the total data set are also impacted by the
186 total number of data blocks. However, when there are a total of 1,000 data blocks, the variation in the
187 performance metrics as a function of the percentage of contaminated data present is minimal. With at least
188 300 total blocks, as might be recommended, the variation is greatly reduced. Note that a critical value of
189 the percentage of contaminated blocks appears to exist between 50% and 75% where the behavior of the
190 performance metrics changes.

191 4. Experimental Results

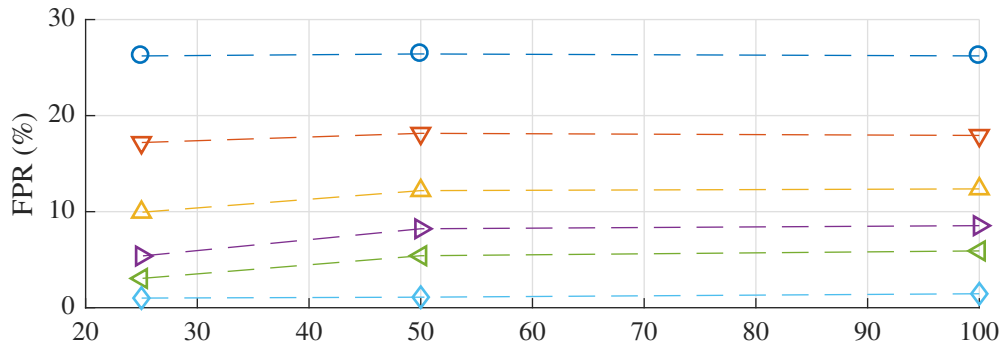
192 The transient classification procedure is applied to an advanced aircraft noise study conducted at the
193 NASA Langley Research Center's 14- by 22-Foot Subsonic Tunnel.¹⁰ A photograph of an example test
194 configuration from this study is shown in Fig. 5, where a hybrid wing body model is installed inverted in the
195 facility test section. As shown in the photograph, microphones are installed on sideline traversing towers,
196 as well as a truss and array panel located above the facility test section.

197 NASA Langley's 14- by 22-Foot Subsonic Wind Tunnel is, by design, an aerodynamic wind tunnel
198 which can operate in an open test section configuration. While significant acoustic improvements have been
199 applied to the facility, measurement microphones are, under some installation configurations, close enough to
200 the open-jet shear layer that hydrodynamic gusts may contaminate the out-of-flow acoustic measurements.
201 This was primarily observed when microphones were at the far-downstream end of the test section, although
202 occasional gust impingement was seen at other measurement stations.

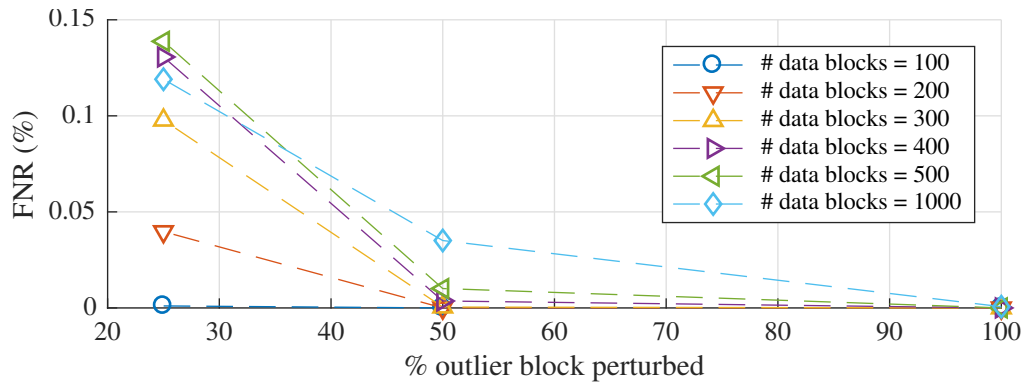
203 An extreme example of gust impingement from the airframe noise component of the test is shown in
204 Fig. 6. The plotted data are for an acquisition where one of the speakers embedded in the model body was
205 driven with a random noise signal which was bandpass filtered to span a frequency range of 4 kHz to 16



(a) accuracy

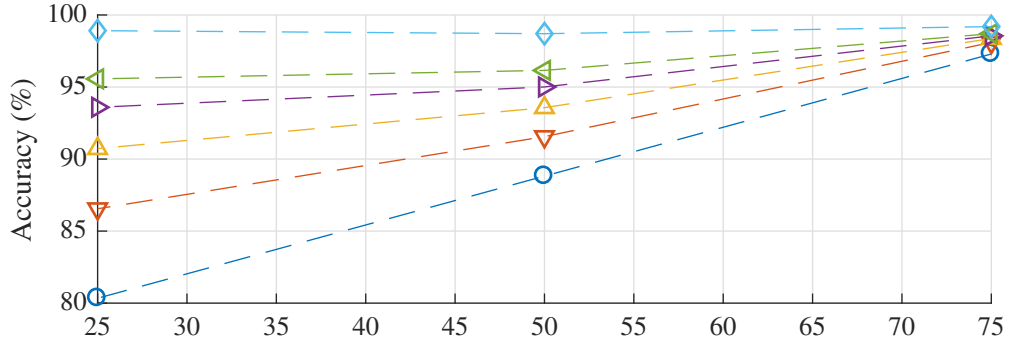


(b) FPR

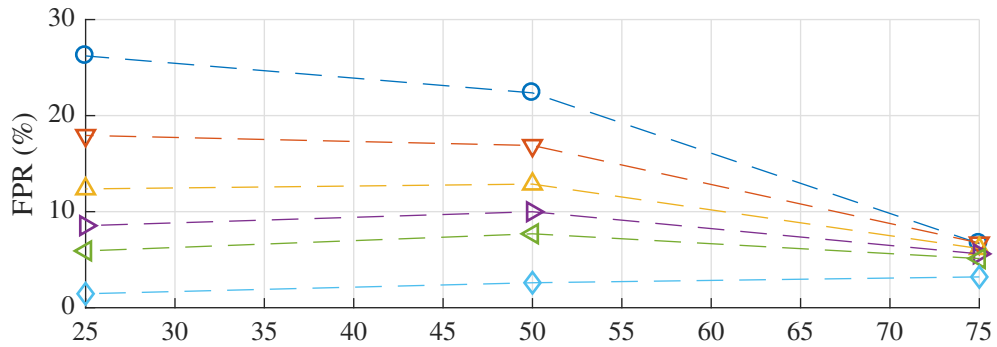


(c) FNR

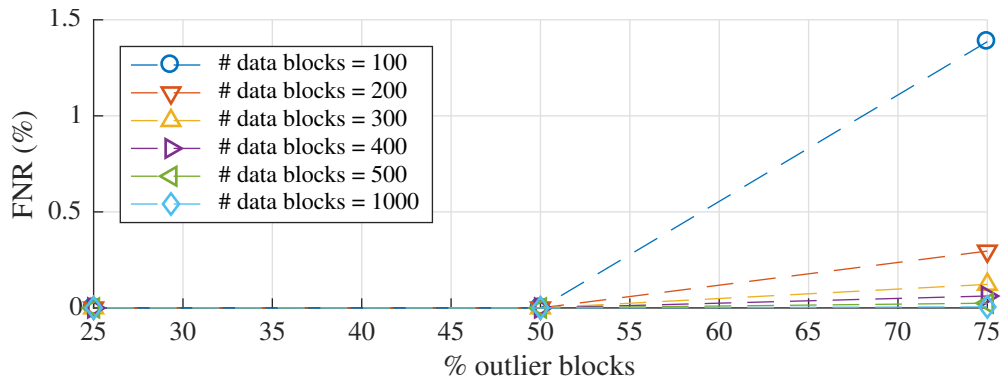
Figure 3. Performance metrics varying the percentage of the contaminated block that is perturbed from the contamination signal while holding the variance ratio to 2, the number of data points per block to $N = 8,192$ points, and percentage of contaminated blocks to 25%.



(a) accuracy



(b) FPR



(c) FNR

Figure 4. Performance metrics varying the percent of data blocks that are contaminated while holding the variance ratio to 2, the number of data points per block to $N = 8,192$ points, and percentage of the data points in the data block perturbed by contamination to 25%.

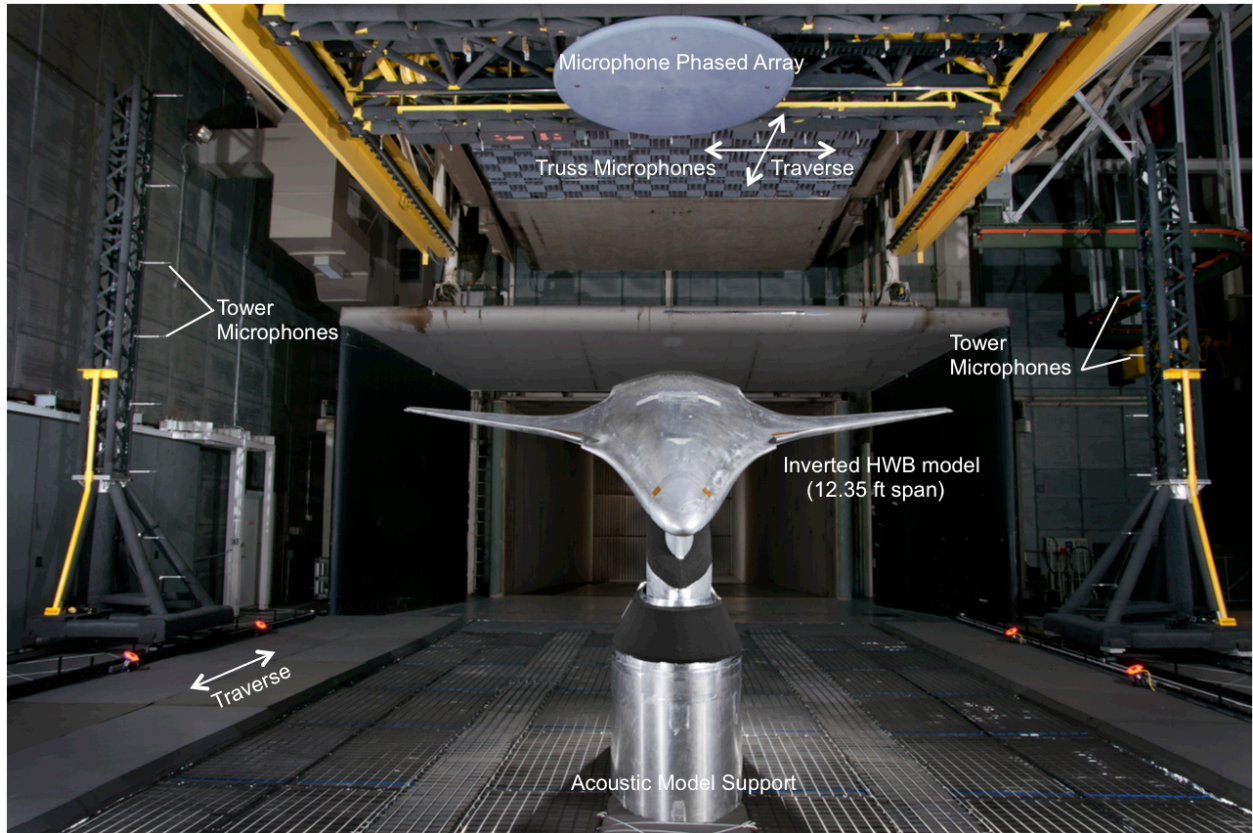


Figure 5. Example arrangement of a hybrid wing body model, phased array and tower traverses.

206 kHz. The hybrid wing body model was pitched to an angle of attack of 14.5° , and the test section Mach
 207 number was $M = 0.23$. The acoustic measurement hardware was traversed to the far-downstream end of
 208 the test section. As shown by the time series in Fig. 6a, the array center microphone signal appears as
 209 might be expected for a stationary, band-limited random signal. The south tower microphone, located in
 210 the upper-right-hand corner of the picture in Fig. 5, clearly experiences extreme transient bursts as shown
 211 in Fig. 6b. The corresponding autospectra are shown in Figs. 6c and 6d. While the array center microphone
 212 spectrum shows the low frequency content of the signal at 4 kHz, the south tower microphone spectrum is
 213 masked by the low frequency content of the burst. Note that at this stage of processing, two clean signals
 214 would not overlay due to differences in propagation distance between the source and each microphone, along
 215 with the speaker directivity. Also, this test is a prime example of why an automated classification method
 216 is desirable. The contamination in the data is clear and could readily be separated manually. However,
 217 roughly a quarter of a million time series records were generated during the test. Manual inspection of such
 218 a volume of data is unreasonable.

219 For these data, the procedure developed for transient classification is applied by breaking the microphone
 220 time series into 920 blocks of desired length $N = 8192$ points. This corresponds to the baseline processing

221 parameters used in the test for spectral analysis.¹¹ The minimum number of accepted blocks is set to 100
222 based on observation of the spectral convergence. A histogram of the south tower microphone data block
223 variances is shown with respect to the left axis in Fig. 7, with the 16 most energetic blocks removed from the
224 plot. Even without these blocks, which would extend the plot abscissa beyond a variance of 500 Pa², this
225 histogram shows a long, thin tail in the direction of large variance values. The corresponding probability
226 density functions for the median- and mean-based models are shown with respect to the right axis in the
227 figure.

228 Of the 920 input blocks, 567 are rejected. The computed $|K|$ as a function of block count used to
229 separate the blocks is shown in Fig. 8, showing an obvious minimum. It should be noted that while this is
230 a large portion of the data to reject, this microphone acquisition is from a location normally outside of the
231 bounds of reasonable acoustic measurement positions in the facility. The histogram of the remaining block
232 variances is shown in Fig. 9, along with the median- and mean-based probability density function estimates
233 for the retained block set. As expected, the probability density functions overlay for the minimum value of
234 $|K|$. The output of the procedure is shown in Figs. 10a and 10b. Visually, the technique has identified and
235 removed the obvious contamination from the time series. In the spectral analysis, the 4 kHz content of the
236 signal is now visible, with a reduction of up to 10 dB in the microphone autospectrum at lower frequencies.
237 Higher frequencies are unaffected.

238 5. Summary & Conclusions

239 An automated method for classifying transient data segments which contaminate stationary acoustic
240 data is presented. The method requires two assumptions. First, it treats the underlying stationary signal
241 of interest as having Gaussian random characteristics. Second, it assumes that contaminated segments of
242 data will have higher variance than clean segments of data. Under these assumptions, it is an unsupervised
243 method which performs binary classification: either a data block is contaminated by a transient signal or it
244 is clean.

245 An extensive set of simulations covering a broad range of conditions shows that the technique has a
246 high degree of accuracy as long as at least 300 data blocks are used, though 500 may be preferable. The
247 FPR may still be greater than 5% under some of the simulated circumstances. However, falsely classifying
248 a few blocks of stationary data as transient and discarding them is not problematic. Wind tunnel time
249 is expensive, so data records have a practical duration limit based on cost. Regardless, standard spectral
250 estimation techniques will still perform well if a few extra blocks are discarded while hundreds are retained.
251 Simulations suggest the technique has a very low FNR for the parameter space explored, so misclassifying
252 enough transient data as stationary to noticeably contaminate a spectral estimate is unlikely.

253 Experimental results from a worst-case scenario in an aeroacoustic wind tunnel test show that, visually,

254 the method succeeds in separating contaminated blocks from the baseline signal of interest. Spectral estima-
255 tion of the signal both before and after the application of the technique shows up to a 10 dB improvement
256 in signal-to-noise ratio due to the removal of contamination. Features in the acoustic spectrum which are
257 masked in the baseline data set are revealed once the transient blocks are removed.

258 **Acknowledgments**

259 The authors would like to acknowledge the support provided by the 14- by 22- Foot Subsonic Tunnel
260 team, by colleagues in the Aeroacoustics and Advanced Sensing & Optical Measurements branches at NASA
261 Langley Research Center, and by colleagues in the Aerodynamics, Noise, and Propulsion Laboratory in the
262 Boeing Test & Evaluation organization at The Boeing Company. The hybrid wing body test was funded by
263 the NASA Environmentally Responsible Aviation Project.

264 **References**

- 265 [1] P. T. Soderman, C. S. Allen, Microphone measurements in and out of airstream, in: T. J. Mueller (Ed.), *Aeroacoustic*
266 *Measurements*, Springer-Verlag, Berlin, Heidelberg, New York, 2002, pp. 22–24.
- 267 [2] W. M. Humphreys, T. F. Brooks, W. W. Hunter, K. R. Meadows, Design and use of microphone directional arrays for
268 aeroacoustic measurements, AIAA-98-0471, 36th AIAA Aerospace Sciences Meeting & Exhibit, Reno, NV, 1998.
- 269 [3] C. J. Bahr, W. C. Horne, Subspace-based background subtraction applied to aeroacoustic wind tunnel testing, *International*
270 *Journal of Aeroacoustics* 16 (2017) 299–325.
- 271 [4] M. Zelen, N. C. Severo, Probability functions, in: M. Abramowitz, I. A. Stegun (Eds.), *Handbook of Mathematical*
272 *Functions*, Dover Publications, Inc., New York, 1972, pp. 940–943.
- 273 [5] 1.3.6.6.11. Gamma Distribution, NIST/SEMATECH e-Handbook of Statistical Methods,
274 <http://www.itl.nist.gov/div898/handbook/>.
- 275 [6] J. S. Bendat, A. G. Piersol, *Random Data Analysis and Measurement Procedures*, John Wiley & Sons, Inc., New York,
276 NY, 2000, 3rd edition, p. 311.
- 277 [7] J. Zhang, Reducing bias of the maximum likelihood estimator of shape parameter for the gamma distribution, *Compu-*
278 *tational Statistics* 28 (2013) 1715–1724.
- 279 [8] J. Cardoso, Infomax and maximum likelihood for blind source separation, *IEEE Signal Processing Letters* 4 (1997)
280 112–114.
- 281 [9] K. M. Ting, Confusion matrix, in: C. Sammut, G. I. Webb (Eds.), *Encyclopedia of Machine Learning*, Springer US,
282 Boston, MA, 2010, p. 209.
- 283 [10] S. L. Heath, T. F. Brooks, F. V. Hutcheson, M. J. Doty, C. J. Bahr, D. Hoad, L. E. Becker, W. M. Humphreys, C. L.
284 Burley, D. J. Stead, D. S. Pope, T. B. Spalt, D. H. Kuchta, G. E. Plassman, J. A. Moen, *NASA Hybrid Wing Body*
285 *Aircraft Aeroacoustic Test Documentation Report*, Technical Report NASA TM-2016-219185, 2016.
- 286 [11] C. J. Bahr, T. F. Brooks, W. M. Humphreys, T. B. Spalt, D. J. Stead, Acoustic data processing and transient signal analysis
287 for the hybrid wing body 14- by 22-foot subsonic wind tunnel test, AIAA 2014-2345, 20th AIAA/CEAS Aeroacoustics
288 Conference, AIAA Aviation 2014, Atlanta, GA, 2014.

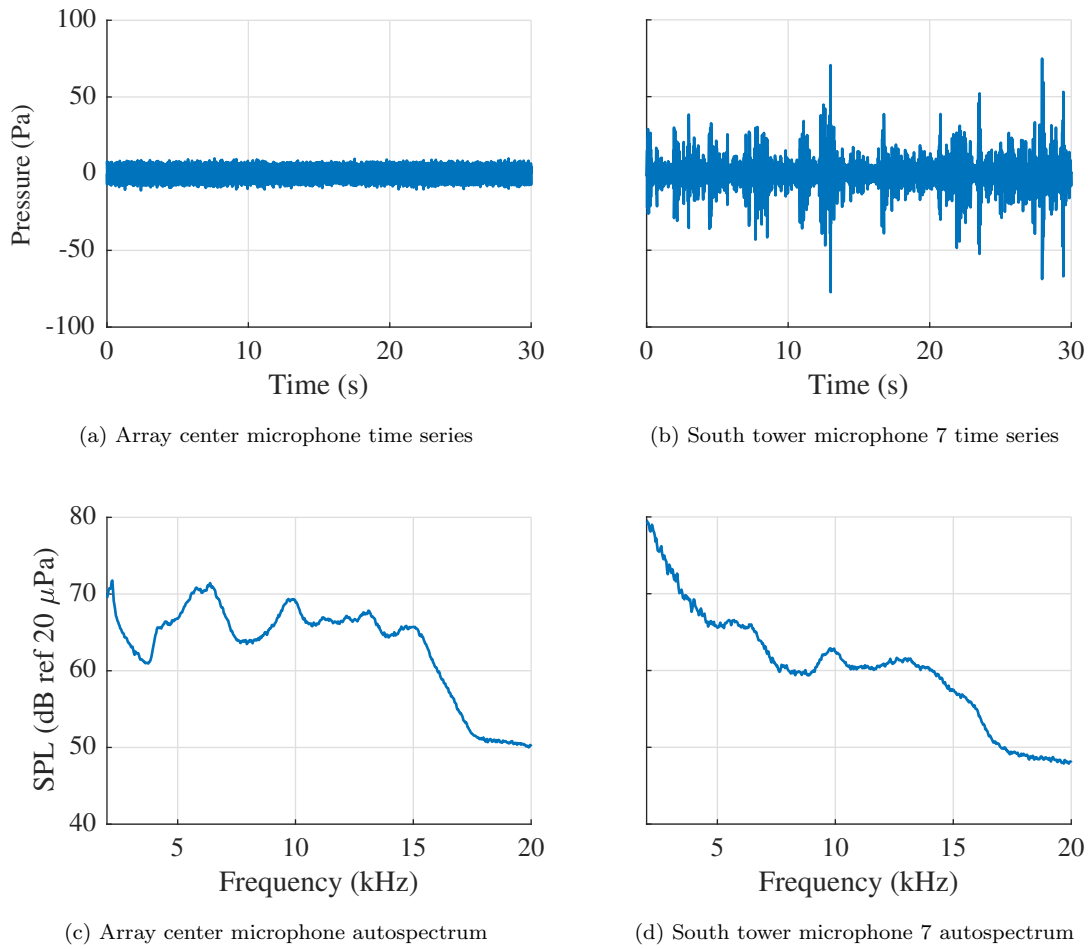


Figure 6. Example data contamination by hydrodynamic impingement. The two compared microphones observed a calibration signal with an output band of 4 kHz to 16 kHz, emitted by one of the model embedded speakers. The hybrid wing body model was at an angle of attack of 14.5° , and the test section Mach number was $M = 0.23$. Acoustic hardware were at the far downstream traverse location. Spectral binwidths are 30.5 Hz.

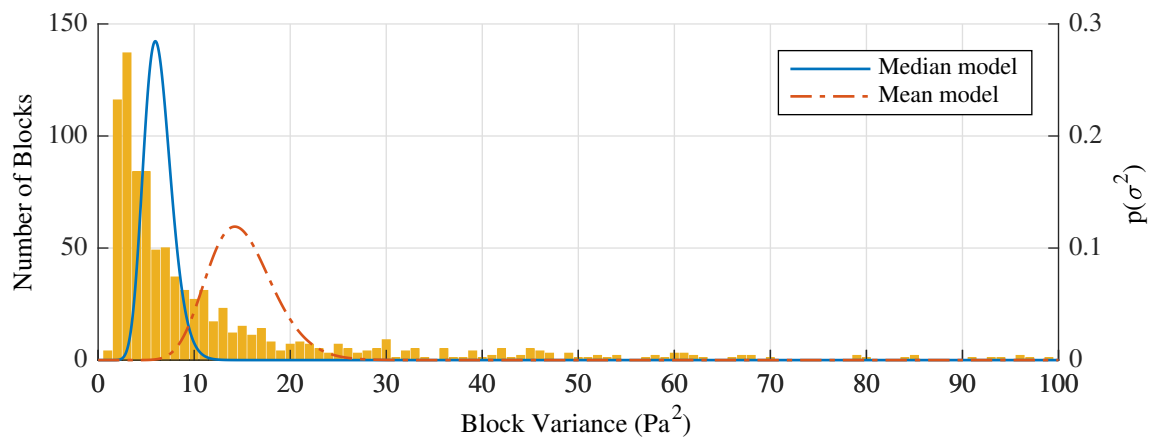


Figure 7. Histogram of block variances from the south tower time series in Fig. 6 excluding the 16 most energetic blocks, and modeled data probability density functions.

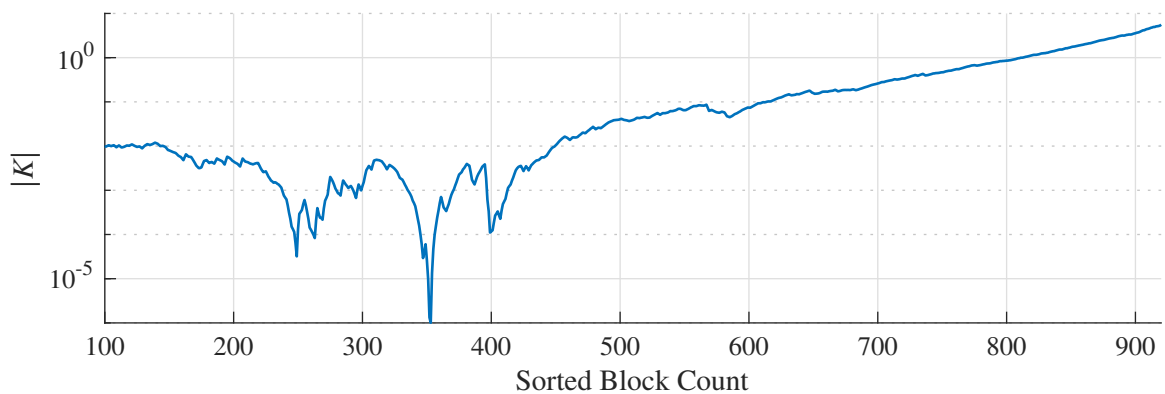


Figure 8. Kullback-Leibler divergence as a function of included block count for the south tower time series data.

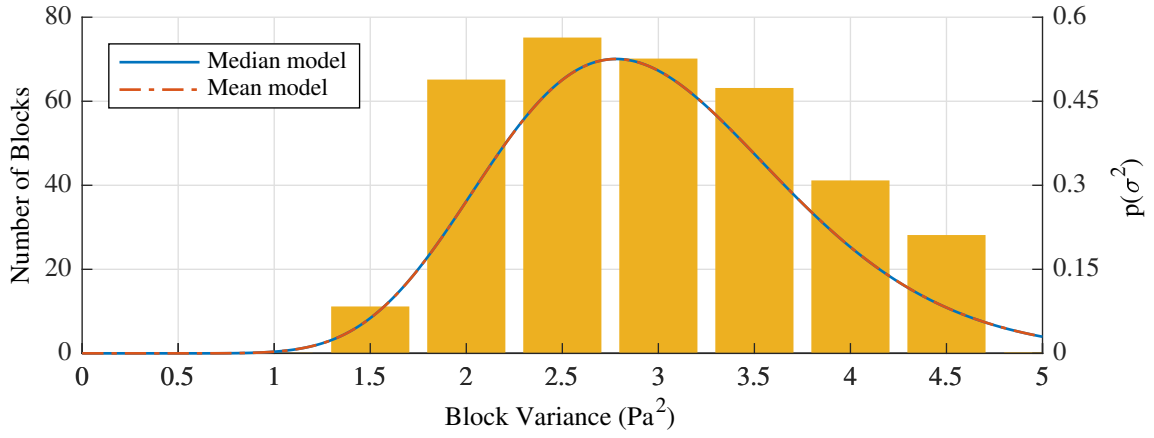
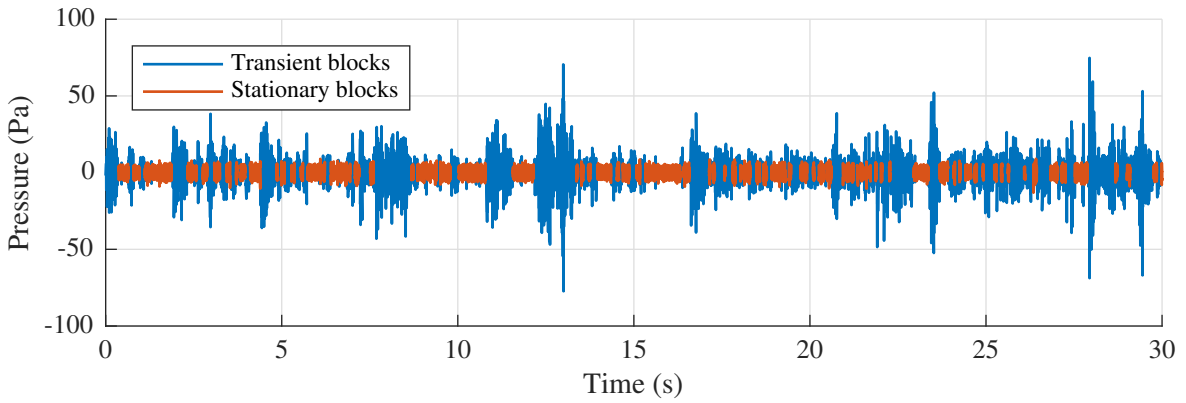
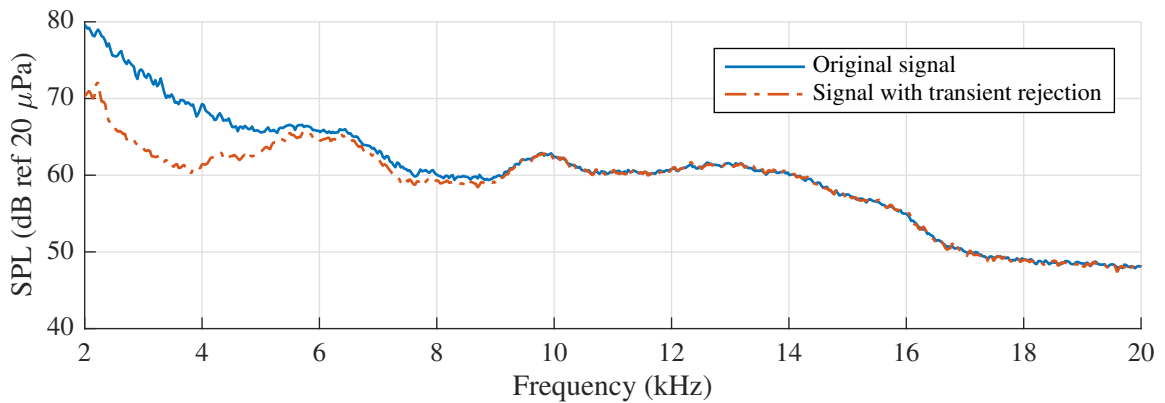


Figure 9. Post-classification histogram of south tower time series data from Fig. 7, along with post-rejection models (mean model almost completely overlays the median model).



(a) Blocks accepted and rejected by the algorithm



(b) Effect of transient block rejection on microphone autospectrum

Figure 10. Results of transient rejection algorithm when applied to the south tower time series data from Fig. 6b. Data blocks are plotted as a function of time. The shift in the estimated data autospectrum is shown. Spectral binwidths are 30.5 Hz.